

**Carbon trends from
thermal and optical
measurements in the
IMPROVE network**

L.-W. A. Chen et al.

This discussion paper is/has been under review for the journal Atmospheric Measurement Techniques (AMT). Please refer to the corresponding final paper in AMT if available.

Consistency of long-term elemental carbon trends from thermal and optical measurements in the IMPROVE network

L.-W. A. Chen^{1,2}, J. C. Chow^{1,2}, J. G. Watson^{1,2}, and B. A. Schichtel³

¹Division of Atmospheric Sciences, Desert Research Institute, 2215 Raggio Parkway, Reno, Nevada, 89512, USA

²State Key Laboratory of Loess and Quaternary Geology, Institute of Earth Environment, Chinese Academy of Sciences, 10 Fenghui South Road, Xi'an, 710075, China

³Cooperative Institute for Research in the Atmosphere, Colorado State University, 1375 Campus Delivery, Fort Collins, Colorado, 80523, USA

Received: 14 April 2012 – Accepted: 8 May 2012 – Published: 31 May 2012

Correspondence to: L.-W. A. Chen (antony@dri.edu)

Published by Copernicus Publications on behalf of the European Geosciences Union.

[Title Page](#)

[Abstract](#)

[Introduction](#)

[Conclusions](#)

[References](#)

[Tables](#)

[Figures](#)

[⏪](#)

[⏩](#)

[◀](#)

[▶](#)

[Back](#)

[Close](#)

[Full Screen / Esc](#)

[Printer-friendly Version](#)

[Interactive Discussion](#)

Abstract

Decreasing trends of elemental carbon (EC) have been reported at US Interagency Monitoring of Protected Visual Environments (IMPROVE) network since 1990, consistent with the phase-in of cleaner engines, residential biomass burning technologies, and prescribed burning methods. The EC trends from the past decade are cautioned due to an upgrade of IMPROVE carbon analyzers and the thermal/optical analysis protocol since 2005. Filter reflectance (τ_R) values measured as part of the carbon analysis were retrieved from archived data and compared with EC for 65 sites with more complete records from 2000 to 2009. The EC- τ_R relationships show only minor changes of EC quantified by the original and upgraded instruments for most of the IMPROVE samples. EC and τ_R show universal decreasing trends across the US. The EC and τ_R trends are correlated well, with national average downward trends of 4.5 % and 4.1 % (of the 2000–2004 baseline medians) per year, respectively. The consistency between independent EC and τ_R trends adds to the weight-of-evidence that EC reductions are real rather than an artifact of the measurement process.

1 Introduction

Elemental carbon (EC), also known as black carbon (BC) or light-absorbing carbon (LAC), is the dominant aerosol component that absorbs visible radiation in the troposphere (Andreae and Gelencser, 2006). EC aerosols from incomplete fuel combustion are non-spherical and internally mixed with organic carbon (OC) (Chakrabarty et al., 2006a,b). Jacobson (2009) estimates the 100-yr Global Warming Potential (GWP) of EC + OC from fossil- and bio-fuel combustion to be 800–1300 relative to carbon dioxide (CO₂). Reducing EC emissions could be a short-term and cost-effective method for slowing global warming (Jacobson, 2002; Bond and Sun, 2005), as well as providing co-benefits for public health, visibility, and material damage (Chow and Watson, 2011).

Carbon trends from thermal and optical measurements in the IMPROVE network

L.-W. A. Chen et al.

Title Page

Abstract

Introduction

Conclusions

References

Tables

Figures

⏪

⏩

◀

▶

Back

Close

Full Screen / Esc

Printer-friendly Version

Interactive Discussion

Carbon trends from thermal and optical measurements in the IMPROVE network

L.-W. A. Chen et al.

[Title Page](#)[Abstract](#)[Introduction](#)[Conclusions](#)[References](#)[Tables](#)[Figures](#)[⏪](#)[⏩](#)[◀](#)[▶](#)[Back](#)[Close](#)[Full Screen / Esc](#)[Printer-friendly Version](#)[Interactive Discussion](#)

Long-term monitoring of aerosol chemical composition in the Interagency Monitoring of Protected Visual Environments (IMPROVE) network (Watson, 2002) reveals a decreasing trend in average EC concentrations by over 25 % in the US from 1990 to 2004 (Murphy et al., 2011) as well as decreases of 40–60 % EC for urban and non-urban California sites from 1988 to 2007 (Bahadur et al., 2011a,b; Schichtel et al., 2011). These trends are consistent with emission reduction measures implemented to attain PM_{2.5} and PM₁₀ National Ambient Air Quality Standards for residential wood combustion (Hough and Kowalczyk, 1983; Butler, 1988; Hough et al., 1988), prescribed burning (Riebau and Fox, 2001; Tian et al., 2008), and engine exhaust (Lloyd and Cackette, 2001). Even though IMPROVE data were available through 2009, Murphy et al. (2011) chose to exclude data from 2005 onward owing to potential biases that might be caused by an upgrade in IMPROVE carbon analyzers beginning in 2005. Chow et al. (2007) demonstrated equivalence between measurements made with the original (Chow et al., 1993) and upgraded (Chow et al., 2007, 2011) analyzers for hundreds of samples from a variety of environments. However, average EC concentrations and EC/OC ratios increased at some (but not all) IMPROVE sites from 2004 to 2005, as illustrated in Fig. 1. The objective of this study is to investigate the recent (2000–2009) trends in IMPROVE EC along with those of filter reflectance which serves as an independent surrogate for EC.

The IMPROVE thermal/optical reflectance (TOR) analysis protocol separates EC from OC on filter samples by temperature-dependent volatilization and oxidation. EC is defined as carbon that does not evolve at ~580 °C in an inert helium (He) atmosphere and is subsequently oxidized to CO₂ with the introduction of oxygen (2 %) at higher temperatures, up to 840 °C. A fraction of OC chars in the inert atmosphere, as evidenced by decreases in light (633 nm He-Ne laser) reflected from the aerosol deposit on the filter surface during the analysis. Pyrolyzed OC (POC) is defined as the carbon evolved after oxygen is introduced and before the reflected light intensity returns to its original value. POC is subtracted from apparent EC measurement to yield true EC concentration in the sampled air. When all of the carbon has evolved, the remaining filter is

Carbon trends from thermal and optical measurements in the IMPROVE network

L.-W. A. Chen et al.

Title Page

Abstract

Introduction

Conclusions

References

Tables

Figures

⏪

⏩

◀

▶

Back

Close

Full Screen / Esc

Printer-friendly Version

Interactive Discussion

usually white, similar to the appearance of a blank filter. Non-white filters occasionally occur during dust events, and these are flagged as part of the IMPROVE protocol.

The 2005 carbon analyzer upgrade led to a transition from the IMPROVE to IMPROVE_A protocol. The transition did not change the temperatures plateaus but rather reflected “actual” analysis temperatures that had been implemented since the inception of the IMPROVE network (Chow et al., 2005). The replacement analyzer allows for more precise sample positioning and temperature control, more flexible data acquisition, a higher intensity laser light beam, and lower trace oxygen levels in the inert He atmosphere than did the old analyzer design. It also allows simultaneous monitoring of filter reflectance and transmittance. Since 2005, light transmitted through the filter and aerosol deposit as well as that reflected from the deposit has been used for charring correction. Thermal/optical transmittance (TOT) often reports higher POC and lower EC than TOR. Chen et al. (2004) and Chow et al. (2004) attributed this to charring of organic vapors adsorbed within the filter (Watson et al., 2009; Chow et al., 2010) which attenuate transmittance substantially but have a minor effect on reflectance from the surface deposit.

Optical measurements designed for charring correction provide alternatives for quantifying EC or BC abundances on filters. Filter attenuation using reflected light (τ_R) or transmitted light (τ_T) is defined as:

$$\tau_R = -\ln(R/R_0)$$

$$\tau_T = -\ln(T/T_0)$$

(1)

where R_0 and T_0 are reflectance and transmittance of blank filters, respectively, and R and T are reflectance and transmittance of particle-laden filters (prior to carbon analysis), respectively. τ_R or τ_T can be a practically linear function of the light absorption coefficient (b_{abs}) for filter samples (Lindberg et al., 1999; Quincey, 2007). The widely-deployed aethalometer and particle-soot absorption photometer (PSAP) estimate b_{abs} from τ_T which is then converted to BC using assumed mass absorption efficiencies derived from simultaneous EC measurements (Watson et al., 2005 and

Carbon trends from thermal and optical measurements in the IMPROVE network

L.-W. A. Chen et al.

Title Page

Abstract

Introduction

Conclusions

References

Tables

Figures



Back

Close

Full Screen / Esc

Printer-friendly Version

Interactive Discussion



references therein). b_{abs} and BC based on τ_{R} are also reported (e.g., Edwards et al., 1983; Janssen et al., 2011). τ_{R} could be more variable in estimating b_{abs} than τ_{T} since the angular distribution of reflectance is more sensitive to the chemical composition of particle deposits (Kopp et al., 1999; Petzold and Schönlinner, 2004). Nonlinearity among b_{abs} (or BC), τ_{R} , and τ_{T} increases with higher loading samples (Arnott et al., 2005) though it was shown in Chen et al. (2004) that the linear relationship between reflectance and transmittance holds up to an EC loading equivalent to $\sim 20 \mu\text{g cm}^{-2}$ on a filter or $\sim 2 \mu\text{g m}^{-3}$ in ambient air for IMPROVE network samples (32.7 m^3 of air sampled through a 3.53 cm^2 filter area).

Since τ_{R} , essentially a measurement of the darkness of the filter deposit, was recorded for every IMPROVE sample before, during, and after the analyzer upgrade and is not related to the thermal/optical analysis, it can be used as an independent indicator of EC. Investigating the EC and τ_{R} relationship before and after the upgrade is necessary. This relationship should be site-, and possibly season-specific, considering the diverse environments represented by IMPROVE samples. Furthermore, τ_{R} trends provide an additional verification for observed EC trends.

2 Methodology

Digital thermograms (which record 1 s value for reflectance, temperature, and carbon content) for >83 000 IMPROVE samples acquired by 24-h sampling on every third day from CY2000 through CY2009 were reprocessed to obtain the initial (dark aerosol deposit) and final (white filter) reflectance values. Data recovery varied by site; typically exceeding 92 % for 2005–2009, but ≤ 80 % for 2000–2004 due to deteriorating storage media (floppy disks and CD-ROMs; it was not practical to recover data from the paper documentation). The 65 sites with the longest records and highest data recovery rates are listed in Table 1 and used for subsequent analysis. Each of these sites contains 80–120 samples per year. They represent 25 US geographic regions as described in Table 1 (see Fig. 2 for the site locations). τ_{R} was calculated per Eq. (1)

from a ten-second average of the initial and final reflectance for all samples. The final reflectance represents effective R_0 as all EC has been removed from the filter.

Pre- and post-upgrade τ_R at a particular IMPROVE site are related to EC through a linear model:

$$\begin{aligned} 5 \quad [\text{EC}]_- &= c_- + b_- \times [\tau_R]_- \\ [\text{EC}]_+ &= c_+ + b_+ \times [\tau_R]_+ \end{aligned} \quad (2)$$

where brackets indicate column vectors of EC or τ_R including all pre (-)/post (+) upgrade (on 1 January 2005) data, and c and b are regression coefficients (c : intercept; b : slope). c and b are expected to differ (i.e., $c_+ \neq c_-$ and/or $b_+ \neq b_-$) only if the instrument upgrade introduced a bias in EC that is substantially larger than typical measurement uncertainties. To examine the changes in b and c , Eqs. (3) and (4) are nested into:

$$\begin{pmatrix} [\text{EC}]_- \\ [\text{EC}]_+ \end{pmatrix} = c_- \begin{pmatrix} 1 \\ 1 \end{pmatrix} + \Delta c \begin{pmatrix} 0 \\ 1 \end{pmatrix} + b_- \begin{pmatrix} [\tau_R]_- \\ [\tau_R]_+ \end{pmatrix} + \Delta b \begin{pmatrix} 0 \\ [\tau_R]_+ \end{pmatrix} \quad (3)$$

15 where 1 and 0 are unit and zero column vectors and Δc and Δb represents $c_+ - c_-$ and $b_+ - b_-$, respectively. Meaningful changes in c and b would lead to Δc and Δb that differ from zero at a statistically-significant level (Gujarati, 1970a,b). A robust least-squares regression method that lowers the influence of outliers was applied to determine the coefficients and respective standard errors and p-values in Eq. (5). This is achieved by the Matlab[®] robustfit function with the Huber iterative reweighting algorithm (Dutter and Huber, 1981).

25 Statistical consistency of c and b pre- and post-2005 (i.e., non-significant Δc and Δb) result from relatively small Δc and Δb or large standard errors. The latter would suggest an insufficient correlation between EC and τ_R for τ_R to be a good predictor for EC. Therefore, it is important to investigate the regression's correlation coefficient as well as the fractional changes in b and c , e.g., $\Delta b/b_-$ and $\Delta c/EC_{\text{-med}}$ ($EC_{\text{-med}}$: median

Carbon trends from thermal and optical measurements in the IMPROVE network

L.-W. A. Chen et al.

Discussion Paper | Discussion Paper | Discussion Paper | Discussion Paper | Discussion Paper

| | |
|--------------------------|--------------|
| Title Page | |
| Abstract | Introduction |
| Conclusions | References |
| Tables | Figures |
| ⏪ | ⏩ |
| ◀ | ▶ |
| Back | Close |
| Full Screen / Esc | |
| Printer-friendly Version | |
| Interactive Discussion | |



[EC]₋ concentration). $\Delta c/EC_{-med}$ provides a better evaluation of changes in Δc than $\Delta c/c_-$ since c_- is usually small to near zero. Lower and Thompson (1988) show that [EC]₊ can be related to [EC]₋ by solving Eqs. (3) and (4) after c and b are determined. This relationship would be the best estimate for determining the relationship between [EC]₊ and [EC]₋, given that a direct regression is not possible.

EC and τ_R trends were further assessed using a non-parametric Mann-Kendall (M-K) test (Kendall, 1975; Yue et al., 2002) which examines the sign of slopes for all possible data pairs and determines trend significance from the difference in positive and negative signs. All data acquired in the same year are considered as concurrent measurements (ties) in the test to minimize influence of intra-annual trends such as seasonal variations (Salas, 1993). M-K statistics yield Sen's slope (Sen, 1968; Burn and Hag El-nur, 2002), which is the median slope across all possible data pairs, and its p-value and confidence intervals. Sen's slope provides a more quantitative estimate of the trends. M-K statistics were calculated with Matlab® code provided by Burkey (2009).

3 Results and discussion

The majority of correlation coefficients (r) of EC versus τ_R from Eq. (5) exceed 0.8 (Table S-1, Supplement). Lower r is found for Urban, Appalachia, and Ohio River Valley sites with high EC concentrations, especially Washington D.C. (U1 in Fig. 2; $r = 0.59$) and James River Face Wilderness (A1, $r = 0.67$). Thirty-six of the 65 sites show no changes in regression slope prior to and after 2005 at the 5% significance level (i.e., $p(\Delta b) > 0.05$). Thirty-four of the thirty-six sites, including all Appalachia sites, show no significant changes in regression intercept prior to and after 2005 (i.e., $p(\Delta c) > 0.05$). $p(\Delta c)$ for the remaining two sites (Cape Romain NWR [SE3] and Canyonlands NP [CP6], see Table 1/Fig. 2), though < 0.05 , are still > 0.01 (1% significant level). The absolute values of Δb and Δc for these 36 sites are small, generally within 10% of b_- and EC_{-med} , respectively (Fig. 3). There is no evidence that the instrument upgrade had an effect on EC measurements for samples taken at these sites (Group I).

Carbon trends from thermal and optical measurements in the IMPROVE network

L.-W. A. Chen et al.

Title Page

Abstract

Introduction

Conclusions

References

Tables

Figures

⏪

⏩

◀

▶

Back

Close

Full Screen / Esc

Printer-friendly Version

Interactive Discussion



Carbon trends from thermal and optical measurements in the IMPROVE network

L.-W. A. Chen et al.

Title Page

Abstract

Introduction

Conclusions

References

Tables

Figures

⏪

⏩

◀

▶

Back

Close

Full Screen / Esc

Printer-friendly Version

Interactive Discussion



The other 29 sites are separated into two groups according to Fig. 3. One group (Group II) exhibits negative Δb along with positive Δc . Six sites of Group II have both Δb and Δc that are significantly different from zero ($p < 0.05$), including Brigantine NWR (E1), U1, Lostwood (NP3), UL Bend (NP6), Glacier NP (NR1), and Denali NP (AK1). These sites are located in eastern (E1, U1) and northern states (NP3, NP6, NR1, AK1). The other group (Group III) exhibits positive Δb and mostly negative Δc . Group III contains 8 sites with both Δb and Δc significantly different from zero ($p < 0.05$), including White Pass [NW4], Three Sisters Wilderness [ON4], Mount Hood [ON5], Bliss SP [SN3], Death Valley [D1], Great Basin [G1], Hance Camp at Grand Canyon NP [CP3], and Bridger Wilderness [NR4]), all of which are located in the Western Cordillera of the continental US (Fig. 2). Figure 4 shows examples of EC- τ_R scatter for these groups.

The POC fraction generally increased for samples analyzed beginning in 2005 due to higher purity of the inert He atmosphere and new procedures to assure that purity (Chow et al., 2007, 2011). Even with the reflectance correction, some POC can be mis-classified as EC, thereby increasing the EC fraction. This is more evident when EC/POC ratios are low and would likely move the EC- τ_R regression towards a higher intercept and lower-to-unchanged slope. Figure 3 is not consistent with this effect being dominant, except possibly at a few Group II sites including E1 (exemplified in Fig. 4b).

For Group III samples, low EC values tend to be even lower beginning in 2005 for the same τ_R (e.g., Fig. 4c). The reason for this is unclear, though it might be related to different sensitivities of reflectance measurements between the old and new instruments for low EC levels. The opposite effects apparent in Group II and Group III could occur simultaneously and to some extent cancel each other. To test whether extreme EC values due to special events such as wildfires can bias the robust regression, regressions were recalculated with EC $> 15 \mu\text{g cm}^{-2}$ excluded. The test resulted in only minor changes in regression intercepts and slopes and did not influence the grouping of the 65 sites.

Carbon trends from thermal and optical measurements in the IMPROVE network

L.-W. A. Chen et al.

[Title Page](#)[Abstract](#)[Introduction](#)[Conclusions](#)[References](#)[Tables](#)[Figures](#)[Back](#)[Close](#)[Full Screen / Esc](#)[Printer-friendly Version](#)[Interactive Discussion](#)

Since regression slopes increase or decrease when intercepts decrease or increase (i.e., change in opposite direction), EC_+ may shift higher or lower compared to EC_- depending on site and EC loading. Figure 5 shows, by site, the characteristic EC_+ vs. EC_- relationships between the 10th and 90th EC_- concentration percentiles, which contains 80 % of the samples. The linear relationships were derived from Eqs. (3) and (4) by eliminating the common variable τ_R , as suggested by Lower and Thompson (1988). EC_+ is shown to be within ± 10 % of EC_- for the most part. Larger deviations, e.g., 10–20 % or -10 – -20 %, are seen for $EC_- \leq 3 \mu\text{g cm}^{-2}$. Two extreme outliers are U1 and AK1, which represent the highest and lowest EC IMPROVE environments, respectively. There may be some change in the EC responses of the old and new instruments for high and low extremes.

The robust M-K test confirms decreasing trends of EC from 2000 through 2009 (Fig. 6), with the largest and smallest rate observed at one Appalachia (A2: $-0.021 \mu\text{g m}^{-3} \text{yr}^{-1}$) site and one Central Rockies (CR2: $-0.003 \mu\text{g m}^{-3} \text{yr}^{-1}$) site, respectively. The trends are statistically significant for all 65 sites at the 5 % significance level. This implies 1.3–8.3 % reductions of ambient EC each year (scaled to $EC_{\text{-med}}$ as 2000–2004 is the IMPROVE baseline period). The national average trend, as calculated from the percentage trends weighted by $EC_{\text{-med}}$ at each site, would be -4.5 % per year. With a simple unweighted regression, Fig. S-1 (Supplement) shows median EC decreasing at 3–5 % per year from 2000–2009. Murphy et al. (2011) report a lower value, ~ -2.2 % EC per year, for March 1990–February 2004. Their analysis was based on average rather than median EC concentrations.

Figure 6 also shows significantly decreasing trends ($p < 0.05$) for τ_R at all except one site in the Northwest (NW4, White Pass, Washington) where the p-value for the negative τ_R trend ($-0.099 \text{Mm}^{-1} \text{yr}^{-1}$) is 0.051. The EC and τ_R trends are highly correlated, at $r^2 = 0.9$ and slope = $10 \text{m}^2 \text{g}^{-1}$ (Fig. 7). Washington, DC (U1 site), the only urban site in this dataset, is an outlier where the EC_+ seems much higher than EC_- based on reflectance (Fig. 5), leading to a smaller EC trend than expected from the τ_R trend. The EC trend at U1 contains a large uncertainty, and this may also be the case

for other urban sites. The national average τ_R trend, as scaled to τ_{R-med} is -4.1% per year, also consistent with the national EC trend.

Although subtle changes are found between EC- τ_R relationships pre- and post-2005, the consistency between recent EC and τ_R trends for the majority of IMPROVE sites do not support that such changes have introduced a major or common bias for the EC trends. Environmental changes, probably due to changing EC emissions and year-to-year meteorological variability, are of larger magnitude than measurement method changes. EC concentrations appear to continue decreasing beyond the 1990–2004 period examined by Murphy et al. (2011) at an average rate of $4.1\text{--}4.5\%$ per year. The Regional Haze Rule (U.S. EPA, 1999) has set the goal of returning visibility to natural conditions by 2064. For EC, the natural concentrations are estimated to be $\sim 10\%$ of the 2000–2004 baseline period. At the current rate of progress, this goal should be met by the 2064 deadline.

Supplementary material related to this article is available online at:
<http://www.atmos-meas-tech-discuss.net/5/3837/2012/amtd-5-3837-2012-supplement.pdf>.

Acknowledgements. This work was sponsored in part by the National Park Service IMPROVE Carbon Analysis Contract No. C2350000894, and the US. EPA task number T2350086187. The conclusions are those of the authors and do not necessarily reflect the views of the sponsoring agencies.

AMTD

5, 3837–3859, 2012

Carbon trends from thermal and optical measurements in the IMPROVE network

L.-W. A. Chen et al.

Title Page

Abstract

Introduction

Conclusions

References

Tables

Figures

⏪

⏩

◀

▶

Back

Close

Full Screen / Esc

Printer-friendly Version

Interactive Discussion



References

- Andreae, M. O. and Gelencsér, A.: Black carbon or brown carbon? The nature of light-absorbing carbonaceous aerosols, *Atmos. Chem. Phys.*, 6, 3131–3148, doi:10.5194/acp-6-3131-2006, 2006.
- 5 Arnott, W. P., Hamasha, K., Moosmüller, H., Sheridan, P. J., and Ogren, J. A.: Towards aerosol light-absorption measurements with a 7-wavelength Aethalometer: Evaluation with a photoacoustic instrument and 3-wavelength nephelometer, *Aerosol Sci. Tech.*, 39, 17–29, 2005.
- Bahadur, R., Feng, Y., Russell, L. M., and Ramanathan, V.: Impact of California's air pollution laws on black carbon and their implications for direct radiative forcing, *Atmos. Environ.*, 45, 1162–1167, 2011a.
- 10 Bahadur, R., Feng, Y., Russell, L. M., and Ramanathan, V.: Response to comments on "Impact of California's air pollution laws on black carbon and their implications for direct radiative forcing" by R. Bahadur et al., *Atmos. Environ.*, 45, 4119–4121, 2011b.
- Bond, T. C. and Sun, H. L.: Can reducing black carbon emissions counteract global warming?, *Environ. Sci. Technol.*, 39, 5921–5926, 2005.
- 15 Burkey, J.: Mann-Kendall Tau-b with Sen's Method (enhanced Matlab code), <http://www.mathworks.com/matlabcentral/fileexchange/11190-mann-kendall-tau-b-with-sens-method-enhanced> (last access: 28 May 2012), 2009.
- 20 Burn, D. H. and Hag Elnur, M. A.: Detection of hydrologic trends and variability, *J. Hydrol.*, 255, 107–122, 2002.
- Butler, A. T.: Control of woodstoves by state regulation as a fine particulate control strategy, in: *Transactions, PM₁₀: Implementation of Standards*, edited by: Mathai, C. V. and Stonefield, D. H., Air Pollution Control Association, Pittsburgh, PA, 654–663, 1988.
- 25 Chakrabarty, R. K., Moosmüller, H., Arnott, W. P., Garro, M. A., and Walker, J.: Structural and fractal properties of particles emitted from spark ignition engines, *Environ. Sci. Technol.*, 40, 6647–6654, 2006a.
- Chakrabarty, R. K., Moosmüller, H., Garro, M. A., Arnott, W. P., Walker, J., Susott, R. A., Babbitt, R. E., Wold, C. E., Lincoln, E. N., and Hao, W. M.: Emissions from the laboratory combustion of wildland fuels: Particle morphology and size, *J. Geophys. Res.-Atmos.*, 111, D07204, doi:10.1029/2005JD006659, 2006b.
- 30

Carbon trends from thermal and optical measurements in the IMPROVE network

L.-W. A. Chen et al.

Title Page

Abstract

Introduction

Conclusions

References

Tables

Figures

◀

▶

◀

▶

Back

Close

Full Screen / Esc

Printer-friendly Version

Interactive Discussion



Carbon trends from thermal and optical measurements in the IMPROVE network

L.-W. A. Chen et al.

Title Page

Abstract

Introduction

Conclusions

References

Tables

Figures

◀

▶

◀

▶

Back

Close

Full Screen / Esc

Printer-friendly Version

Interactive Discussion



Chen, L.-W. A., Chow, J. C., Watson, J. G., Moosmüller, H., and Arnott, W. P.: Modeling reflectance and transmittance of quartz-fiber filter samples containing elemental carbon particles: Implications for thermal/optical analysis, *J. Aerosol Sci.*, 35, 765–780, 2004.

Chow, J. C. and Watson, J. G.: Air quality management of multiple pollutants and multiple effects, *Air Qual. Clim. Change J.*, 45, 26–32, 2011.

Chow, J. C., Watson, J. G., Pritchett, L. C., Pierson, W. R., Frazier, C. A., and Purcell, R. G.: The DRI Thermal/Optical Reflectance carbon analysis system: Description, evaluation and applications in U.S. air quality studies, *Atmos. Environ.*, 27A, 1185–1201, 1993.

Chow, J. C., Watson, J. G., Chen, L.-W. A., Arnott, W. P., Moosmüller, H., and Fung, K. K.: Equivalence of elemental carbon by Thermal/Optical Reflectance and Transmittance with different temperature protocols, *Environ. Sci. Technol.*, 38, 4414–4422, 2004.

Chow, J. C., Watson, J. G., Chen, L.-W. A., Paredes-Miranda, G., Chang, M.-C. O., Trimble, D., Fung, K. K., Zhang, H., and Zhen Yu, J.: Refining temperature measures in thermal/optical carbon analysis, *Atmos. Chem. Phys.*, 5, 2961–2972, doi:10.5194/acp-5-2961-2005, 2005.

Chow, J. C., Watson, J. G., Chen, L.-W. A., Chang, M. C. O., Robinson, N. F., Trimble, D. L., and Kohl, S. D.: The IMPROVE.A temperature protocol for thermal/optical carbon analysis: Maintaining consistency with a long-term database, *J. Air Waste Manage. Assoc.*, 57, 1014–1023, 2007.

Chow, J. C., Watson, J. G., Chen, L.-W. A., Rice, J., and Frank, N. H.: Quantification of PM_{2.5} organic carbon sampling artifacts in US networks, *Atmos. Chem. Phys.*, 10, 5223–5239, doi:10.5194/acp-10-5223-2010, 2010.

Chow, J. C., Watson, J. G., Robles, J., Wang, X. L., Chen, L.-W. A., Trimble, D. L., Kohl, S. D., Tropp, R. J., and Fung, K. K.: Quality assurance and quality control for thermal/optical analysis of aerosol samples for organic and elemental carbon, *Anal. Bioanal. Chem.*, 401, 3141–3152, 2011.

Dutter, R. and Huber, P. J.: Numerical methods for the non linear robust regression problem, *J. Stat. Comput. Simul.*, 13, 79–113, 1981.

Edwards, J. D., Ogren, J. A., Weiss, R. E., and Charlson, R. J.: Particulate air pollutants: A comparison of British “Smoke” with optical absorption coefficients and elemental carbon concentration, *Atmos. Environ.*, 17, 2337–2341, 1983.

Gujarati, D.: Use of dummy variables in testing for equality between sets of coefficients in two linear regressions: A generalization, *Am. Stat.*, 24, 18–22, 1970a.

Carbon trends from thermal and optical measurements in the IMPROVE network

L.-W. A. Chen et al.

Title Page

Abstract

Introduction

Conclusions

References

Tables

Figures

◀

▶

◀

▶

Back

Close

Full Screen / Esc

Printer-friendly Version

Interactive Discussion



- Gujarati, D.: Use of dummy variables in testing for equality between sets of coefficients in two linear regressions: A note, *Am. Stat.*, 24, 50–52, 1970b.
- Hough, M. L. and Kowalczyk, J. F.: A comprehensive strategy to reduce residential wood burning impacts in small urban communities, *J. Air Poll. Control Assoc.*, 33, 1121–1125, 1983.
- 5 Hough, M. L., Tomblason, B., and Wolgamott, M.: Oregon approach to reducing residential woodsmoke as part of the PM₁₀ strategy, in: *Transactions, PM₁₀: Implementation of Standards*, edited by: Mathai, C. V. and Stonefield, D. H., Air Pollution Control Association, Pittsburgh, PA, 646–653, 1988.
- Jacobson, M. Z.: Control of fossil-fuel particulate black carbon plus organic matter, possibly the most effective method of slowing global warming, *J. Geophys. Res.*, 107, 4410, doi:10.1029/2001JD001376, 2002.
- 10 Jacobson, M. Z.: Testimony for U.S. Environmental Protection Agency Public Hearing on the Proposed Endangerment and Cause or Contribute Findings for Greenhouse Gases Under the Clean Air Act, <http://www.stanford.edu/group/efmh/jacobson/PDF%20files/EPAEndang0509.pdf> (last access: 28 May 2012), 18 May 2009.
- 15 Janssen, N. A. H., Hoek, G., Simic-Lawson, M., Fischer, P., van Bree, L., Ten Brink, H., Keuken, M., Atkinson, R. W., Anderson, H. R., Brunekreef, B., and Cassee, F. R.: Black carbon as an additional indicator of the adverse health effects of airborne particles compared with PM₁₀ and PM_{2.5}, *Environ. Health Perspect.*, 119, 1691–1699, 2011.
- 20 Kendall, M. G.: *Rank Correlation Methods*, Griffin, London, UK, 1975.
- Kopp, C., Petzold, A., and Niessner, R.: Investigation of the specific attenuation cross-section of aerosols deposited on fiber filters with a polar photometer to determine black carbon, *J. Aerosol Sci.*, 30, 1153–1163, 1999.
- Lindberg, J. D., Douglass, R. E., and Garvey, D. M.: Atmospheric particulate absorption and black carbon measurement, *Appl. Optics*, 38, 2369–2376, 1999.
- 25 Lloyd, A. C. and Cackette, T. A.: Critical review – Diesel engines: Environmental impact and control, *J. Air Waste Manage. Assoc.*, 51, 809–847, 2001.
- Lower, W. R. and Thompson, W. A.: An indirect test of correlation, *Environ. Toxicol. Chem.*, 7, 77–80, 1988.
- 30 Murphy, D. M., Chow, J. C., Leibensperger, E. M., Malm, W. C., Pitchford, M., Schichtel, B. A., Watson, J. G., and White, W. H.: Decreases in elemental carbon and fine particle mass in the United States, *Atmos. Chem. Phys.*, 11, 4679–4686, doi:10.5194/acp-11-4679-2011, 2011.

Carbon trends from thermal and optical measurements in the IMPROVE network

L.-W. A. Chen et al.

Title Page

Abstract

Introduction

Conclusions

References

Tables

Figures

◀

▶

◀

▶

Back

Close

Full Screen / Esc

Printer-friendly Version

Interactive Discussion



- Petzold, A. and Schönlinner, M.: Multi-angle absorption photometry – A new method for the measurement of aerosol light absorption and atmospheric black carbon, *J. Aerosol Sci.*, 35, 421–441, 2004.
- 5 Quincey, P. G.: A relationship between Black Smoke Index and Black Carbon concentration, *Atmos. Environ.*, 41, 7964–7968, 2007.
- Riebau, A. R. and Fox, D.: The new smoke management, *Inter. J. Wildland Fire*, 10, 415–427, 2001.
- Salas, J. D.: Analysis and modeling of hydrologic time series, in: *Handbook of Hydrology*, edited by: Maidment, D. R., McGraw-Hill, Columbus, OH, 19.1–19.63, 1993.
- 10 Schichtel, B. A., Pitchford, M. L., and White, W. H.: Comments on “Impact of California’s Air Pollution Laws on Black Carbon and their Implications for Direct Radiative Forcing” by R. Bahadur et al., *Atmos. Environ.*, 45, 4116–4118, 2011.
- Sen, P. K.: Estimates of the regression coefficient based on Kendall’s tau, *J. Amer. Stat. Assoc.*, 63, 1379–1389, 1968.
- 15 Tian, D., Wang, Y. H., Bergin, M., Hu, Y. T., Liu, Y. Q., and Russell, A. G.: Air quality impacts from prescribed forest fires under different management practices, *Environ. Sci. Technol.*, 42, 2767–2772, 2008.
- U.S. EPA: 40 CFR Part 51 – Regional haze regulations: Final rule, Federal Register, Environmental Protection Agency, Washington, DC, 64, 35714–35774, 1999.
- 20 Watson, J. G.: Visibility: Science and regulation – 2002 Critical Review, *J. Air Waste Manage. Assoc.*, 52, 628–713, 2002.
- Watson, J. G., Chow, J. C., and Chen, L.-W. A.: Summary of organic and elemental carbon/black carbon analysis methods and intercomparisons, *Aerosol Air Qual. Res.*, 5, 65–102, 2005.
- 25 Watson, J. G., Chow, J. C., Chen, L.-W. A., and Frank, N. H.: Methods to assess carbonaceous aerosol sampling artifacts for IMPROVE and other long-term networks, *J. Air Waste Manage. Assoc.*, 59, 898–911, 2009.
- Yue, S., Pilon, P., and Cavadias, G.: Power of the Mann-Kendall and Spearman’s rho tests for detecting monotonic trends in hydrological series, *J. Hydrol.*, 259, 254–271, 2002.

Table 1. Region, location, and data completeness (2000–2009) of EC and τ_R for 65 IMPROVE sites selected for this study.

| Regions | Location | | | Data completeness* | | | | |
|-----------------------|----------|-------|-------------------------------|--------------------|-----------|------------|-----------|-----------|
| | Code | Name | Class I area | Latitude | Longitude | m.s.l. (m) | 2000–2004 | 2005–2009 |
| Northeast | NE1 | MOOS1 | Moosehorn NWR | 45.1259 | -67.2661 | 77 | 73 % | 97 % |
| | NE2 | ACAD1 | Acadia NP | 44.3771 | -68.261 | 157 | 78 % | 99 % |
| East Coast | E1 | BRIG1 | Brigantine NWR | 39.465 | -74.4492 | 5 | 80 % | 95 % |
| Urban | U1 | WASH1 | Washington D.C. | 38.8762 | -77.0344 | 15 | 71 % | 93 % |
| Appalachia | A1 | JARI1 | James River Face Wilderness | 37.6266 | -79.5125 | 289 | 72 % | 99 % |
| | A2 | SIPS1 | Sipsy Wilderness | 34.3433 | -87.3388 | 286 | 72 % | 92 % |
| | A3 | GRSM1 | Great Smoky Mountains NP | 35.6334 | -83.9416 | 810 | 73 % | 98 % |
| | A4 | LIGO1 | Linville Gorge | 35.9723 | -81.9331 | 968 | 72 % | 93 % |
| | A5 | SHEN1 | Shenandoah NP | 38.5229 | -78.4348 | 1079 | 73 % | 97 % |
| | A6 | DOSO1 | Dolly Sods Wilderness | 39.1053 | -79.4261 | 1182 | 74 % | 100 % |
| Southeast | SE1 | CHAS1 | Chassahowitzka NWR | 28.7484 | -82.5549 | 4 | 77 % | 95 % |
| | SE2 | OKEF1 | Okefenokee NWR | 30.7405 | -82.1283 | 48 | 80 % | 98 % |
| | SE3 | ROMA1 | Cape Romain NWR | 32.941 | -79.6572 | 4 | 77 % | 97 % |
| Boundary waters | B1 | SENE1 | Seney | 46.2889 | -85.9503 | 214 | 75 % | 97 % |
| | B2 | ISLE1 | Isle Royale NP | 47.4596 | -88.1491 | 182 | 78 % | 96 % |
| | B3 | VOYA1 | Voyageurs NP #1 | 48.4132 | -92.8303 | 425 | 71 % | 92 % |
| Ohio River valley | O1 | MACA1 | Mammoth Cave NP | 37.1318 | -86.1479 | 235 | 75 % | 99 % |
| Mid south | MS1 | UPBU1 | Upper Buffalo Wilderness | 35.8258 | -93.203 | 722 | 70 % | 95 % |
| | MS2 | CACR1 | Caney Creek | 34.4544 | -94.1429 | 683 | 72 % | 93 % |
| Northern Great Plains | NP1 | WICA1 | Wind Cave | 43.5576 | -103.484 | 1296 | 71 % | 93 % |
| | NP2 | THRO1 | Theodore Roosevelt | 46.8948 | -103.378 | 852 | 70 % | 97 % |
| | NP3 | LOST1 | Lostwood | 48.6419 | -102.402 | 696 | 76 % | 91 % |
| | NP4 | MELA1 | Medicine Lake | 48.4871 | -104.476 | 606 | 70 % | 96 % |
| | NP5 | BADL1 | Badlands NP | 43.7435 | -101.941 | 736 | 74 % | 99 % |
| | NP6 | ULBE1 | UL Bend | 47.5823 | -108.72 | 891 | 75 % | 95 % |
| West Texas | W1 | BIBE1 | Big Bend NP | 29.3027 | -103.178 | 1066 | 70 % | 94 % |
| | W2 | GUMO1 | Guadalupe Mountains NP | 31.833 | -104.809 | 1672 | 78 % | 96 % |
| Central Rockies | CR1 | ROMO2 | Rocky Mountain NP | 40.2783 | -105.546 | 2760 | 74 % | 98 % |
| | CR2 | GRSA1 | Great Sand Dunes NM | 37.7249 | -105.519 | 2498 | 76 % | 93 % |
| | CR3 | WHRI1 | White River NF | 39.1536 | -106.821 | 3413 | 76 % | 96 % |
| Colorado Plateau | CP1 | BRCA1 | Bryce Canyon NP | 37.6184 | -112.174 | 2481 | 74 % | 95 % |
| | CP2 | BAND1 | Bandelier NM | 35.7797 | -106.266 | 1988 | 76 % | 94 % |
| | CP3 | HANC1 | Hance Camp at Grand Canyon NP | 35.9731 | -111.984 | 2267 | 75 % | 96 % |
| | CP4 | WEMI1 | Weminuche Wilderness | 37.6594 | -107.8 | 2750 | 75 % | 99 % |
| | CP5 | MEVE1 | Mesa Verde NP | 37.1984 | -108.491 | 2172 | 72 % | 96 % |
| | CP6 | CANY1 | Canyonlands NP | 38.4587 | -109.821 | 1798 | 71 % | 93 % |
| Southern Arizona | SA1 | CHIR1 | Chiricahua NM | 32.0094 | -109.389 | 1554 | 70 % | 95 % |
| Mogollon Plateau | MP1 | SYCA1 | Sycamore Canyon | 35.1406 | -111.969 | 2046 | 70 % | 94 % |
| | MP2 | IKBA1 | Ike's Backbone | 34.3405 | -111.683 | 1297 | 74 % | 97 % |
| | MP3 | BALD1 | Mount Baldy | 34.0584 | -109.441 | 2508 | 70 % | 96 % |

Carbon trends from thermal and optical measurements in the IMPROVE network

L.-W. A. Chen et al.

Title Page

Abstract Introduction

Conclusions References

Tables Figures

◀ ▶

◀ ▶

Back Close

Full Screen / Esc

Printer-friendly Version

Interactive Discussion



Carbon trends from thermal and optical measurements in the IMPROVE network

L.-W. A. Chen et al.

Title Page

Abstract

Introduction

Conclusions

References

Tables

Figures

⏪

⏩

◀

▶

Back

Close

Full Screen / Esc

Printer-friendly Version

Interactive Discussion



Table 1. Continued.

| Regions | Code | Name | Class I area | Location | | | Data completeness* | |
|------------------------------|------|-------|--------------------------|----------|-----------|------------|--------------------|-----------|
| | | | | Latitude | Longitude | m.s.l. (m) | 2000–2004 | 2005–2009 |
| Northern Rockies | NR1 | GLAC1 | Glacier NP | 48.5105 | −113.997 | 975 | 74 % | 94 % |
| | NR2 | MONT1 | Monture | 47.1222 | −113.154 | 1282 | 70 % | 96 % |
| | NR3 | CABI1 | Cabinet Mountains | 47.9549 | −115.671 | 1441 | 71 % | 95 % |
| | NR4 | BRID1 | Bridger Wilderness | 42.9749 | −109.758 | 2626 | 78 % | 94 % |
| Great Basin | G1 | GRBA1 | Great Basin NP | 39.0052 | −114.216 | 2065 | 70 % | 96 % |
| Southern California | SC1 | SAGO1 | San Gorgonio Wilderness | 34.1939 | −116.913 | 1726 | 71 % | 98 % |
| | SC2 | JOSH1 | Joshua Tree NP | 34.0695 | −116.389 | 1235 | 74 % | 95 % |
| Death Valley | D1 | DEVA1 | Death Valley NP | 36.5089 | −116.848 | 130 | 70 % | 96 % |
| Hell's Canyon | H1 | STAR1 | Starkey | 45.2249 | −118.513 | 1259 | 74 % | 98 % |
| Sierra Nevada | SN1 | SEQU1 | Sequoia NP | 36.4894 | −118.829 | 519 | 72 % | 96 % |
| | SN2 | YOSE1 | Yosemite NP | 37.7133 | −119.706 | 1603 | 75 % | 94 % |
| | SN3 | BLIS1 | Bliss SP (TRPA) | 38.9761 | −120.103 | 2130 | 71 % | 93 % |
| Columbia River Gorge | CG1 | CORI1 | Columbia River Gorge | 45.6644 | −121.001 | 178 | 76 % | 96 % |
| California Coast | CC1 | PINN1 | Pinnacles NM | 36.4833 | −121.157 | 302 | 72 % | 97 % |
| Northwest | NW1 | MORA1 | Mount Rainier NP | 46.7583 | −122.124 | 439 | 75 % | 93 % |
| | NW2 | SNPA1 | Snoqualmie Pass | 47.422 | −121.426 | 1049 | 73 % | 97 % |
| | NW3 | NOCA1 | North Cascades | 48.7316 | −121.065 | 568 | 70 % | 94 % |
| | NW4 | WHPA1 | White Pass | 46.6243 | −121.388 | 1827 | 75 % | 95 % |
| Oregon & Northern California | ON1 | KALM1 | Kalmiopsis | 42.552 | −124.059 | 80 | 80 % | 98 % |
| | ON2 | CRLA1 | Crater Lake NP | 42.8958 | −122.136 | 1996 | 70 % | 94 % |
| | ON3 | LABE1 | Lava Beds NM | 41.7117 | −121.507 | 1459 | 70 % | 95 % |
| | ON4 | THSI1 | Three Sisters Wilderness | 44.291 | −122.043 | 885 | 74 % | 98 % |
| | ON5 | MOHO1 | Mount Hood | 45.2888 | −121.784 | 1531 | 78 % | 97 % |
| | ON6 | REDW1 | Redwood NP | 41.5608 | −124.084 | 243 | 70 % | 94 % |
| Alaska | AK1 | DENA1 | Denali NP | 63.7233 | −148.968 | 658 | 75 % | 96 % |

Complete EC- τ_R pairs, where EC: elemental carbon; τ_R : $-\ln(R/R_0)$ as filter attenuation with respect to reflectance.

Carbon trends from thermal and optical measurements in the IMPROVE network

L.-W. A. Chen et al.

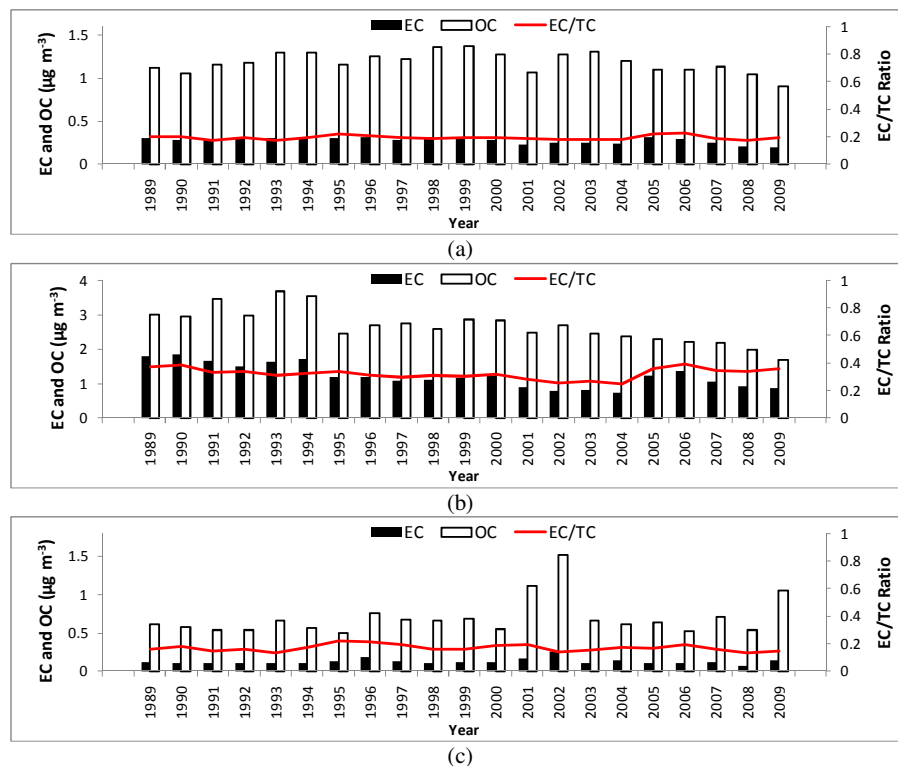


Fig. 1. Annual average organic carbon (OC), elemental carbon (EC), and the ratio of EC to total carbon (TC = OC + EC) for **(a)** all IMPROVE data, **(b)** downtown Washington DC (U1), and **(c)** Bryce Canyon National Park (CP1) since 1989. Data were acquired from the Visibility Information Exchange Web System (VIEWS) website (<http://views.cira.colostate.edu/>). An EC increase from 2004 to 2005 corresponds with the carbon analyzer upgrade for **(a)** and **(b)**, but this is not observed at every site, the **(c)** being one example.

[Title Page](#)
[Abstract](#)
[Introduction](#)
[Conclusions](#)
[References](#)
[Tables](#)
[Figures](#)
[⏪](#)
[⏩](#)
[◀](#)
[▶](#)
[Back](#)
[Close](#)
[Full Screen / Esc](#)
[Printer-friendly Version](#)
[Interactive Discussion](#)

Carbon trends from thermal and optical measurements in the IMPROVE network

L.-W. A. Chen et al.

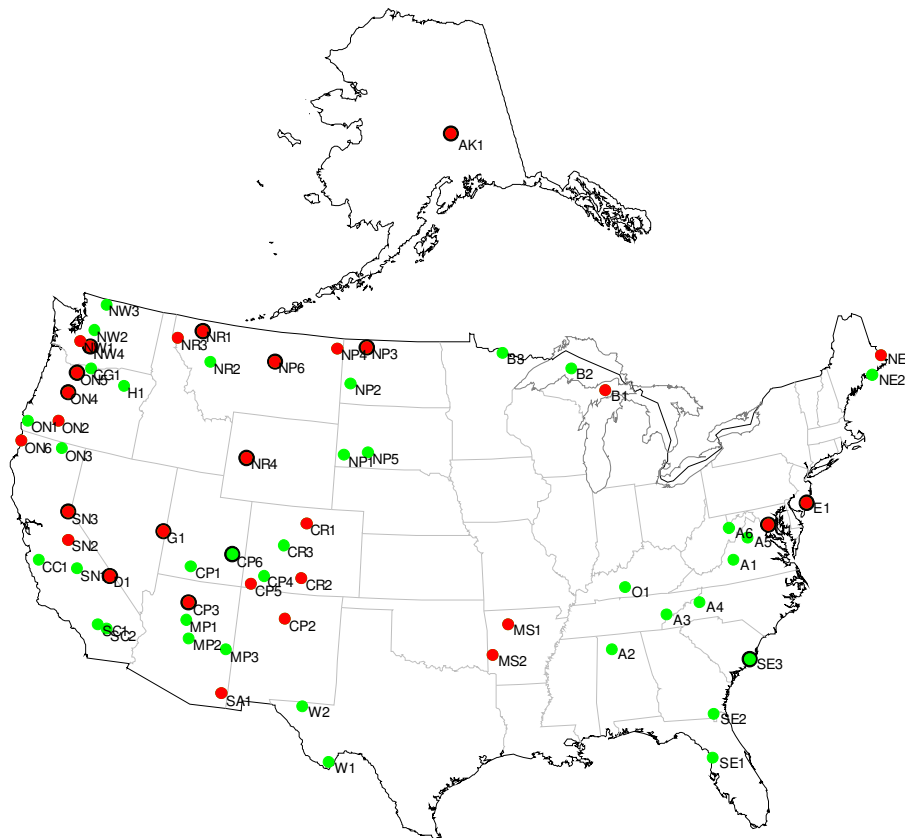


Fig. 2. Sixty-five IMPROVE sites in 25 regions (see Table 1 for definitions). Color codes indicate the changes of $EC-\tau_R$ regression coefficients across the instrumental upgrade in 2005. Red: significant change in slope ($p < 0.05$); solid edge: significant change in intercept ($p < 0.05$); green: all other sites without significant changes. See text for details.

[Title Page](#)
[Abstract](#)
[Introduction](#)
[Conclusions](#)
[References](#)
[Tables](#)
[Figures](#)
[◀](#)
[▶](#)
[◀](#)
[▶](#)
[Back](#)
[Close](#)
[Full Screen / Esc](#)
[Printer-friendly Version](#)
[Interactive Discussion](#)

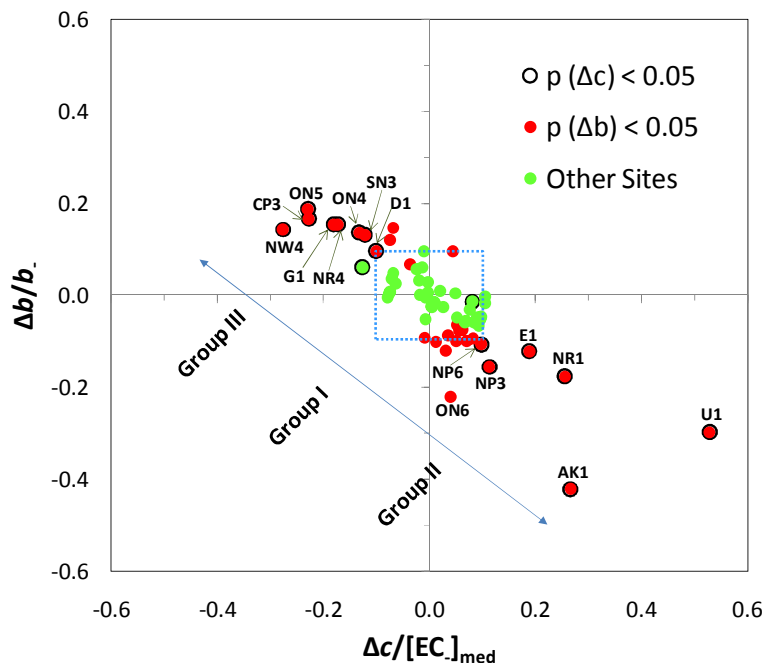


Fig. 3. Changes in $EC-\tau_R$ robust regression intercept (Δc)/slope (Δb) relative to median EC (EC_{-med})/regression slope (b_{-}) prior to 2005. Red: significant change in slope; solid edge: significant change in intercept; green: all other sites without significant changes. Group I consists of 36 sites with Δb not significantly different from zero. Group II consists of 17 sites with negative Δb that are significantly different from zero, and Group III consists of 12 sites with positive Δb that are significantly different from zero.

[Title Page](#)
[Abstract](#)
[Introduction](#)
[Conclusions](#)
[References](#)
[Tables](#)
[Figures](#)
[⏪](#)
[⏩](#)
[◀](#)
[▶](#)
[Back](#)
[Close](#)
[Full Screen / Esc](#)
[Printer-friendly Version](#)
[Interactive Discussion](#)

Carbon trends from thermal and optical measurements in the IMPROVE network

L.-W. A. Chen et al.

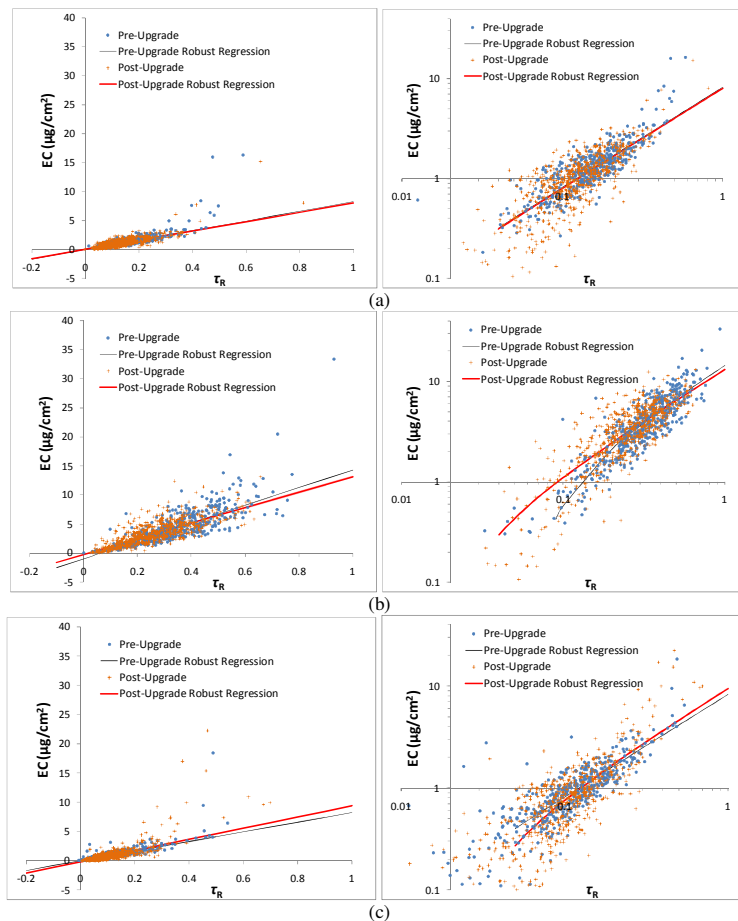


Fig. 4. EC- τ_R scatter for (a) CP4, (b) E1, and (c) CP3 as an example of Group I, II, and III sites, respectively. Pre- and post-upgrade periods are separated for robust regression analysis. Left panels: linear scale; right panels: log scale.

[Title Page](#)
[Abstract](#)
[Introduction](#)
[Conclusions](#)
[References](#)
[Tables](#)
[Figures](#)
[⏪](#)
[⏩](#)
[⏴](#)
[⏵](#)
[Back](#)
[Close](#)
[Full Screen / Esc](#)
[Printer-friendly Version](#)
[Interactive Discussion](#)

Carbon trends from thermal and optical measurements in the IMPROVE network

L.-W. A. Chen et al.

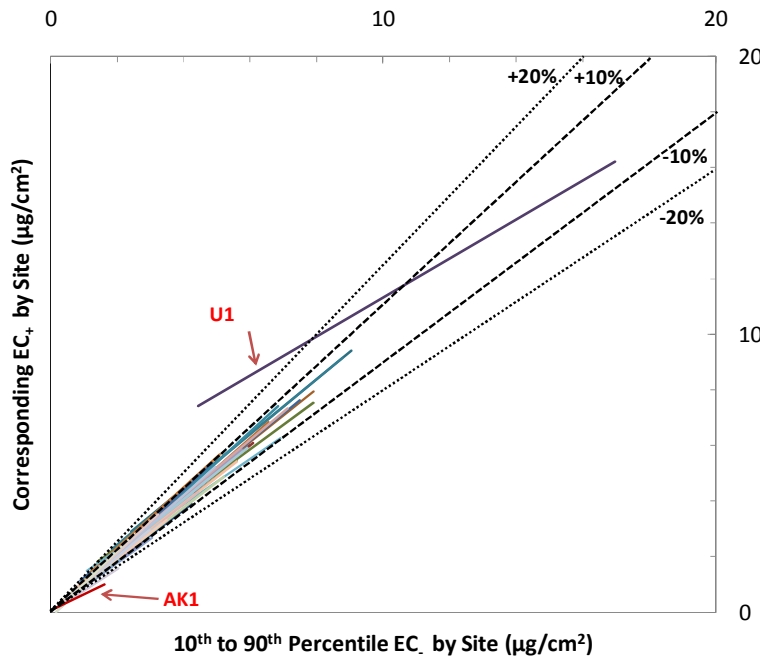


Fig. 5. EC_+ (after upgrade) vs. EC_- (before upgrade) relationships derived from robust regression analysis through τ_R . Relationships of EC_+ and EC_- with τ_R are determined separately, and then EC_+ is related to EC_- by eliminating τ_R in simultaneous equations. Each solid line represents one of the 65 sites stretching from 10th to 90th percentile of EC_- . Dashed lines indicate $\pm 10\%$ or $\pm 20\%$ deviations.

[Title Page](#)
[Abstract](#)
[Introduction](#)
[Conclusions](#)
[References](#)
[Tables](#)
[Figures](#)
[◀](#)
[▶](#)
[◀](#)
[▶](#)
[Back](#)
[Close](#)
[Full Screen / Esc](#)
[Printer-friendly Version](#)
[Interactive Discussion](#)

Carbon trends from thermal and optical measurements in the IMPROVE network

L.-W. A. Chen et al.

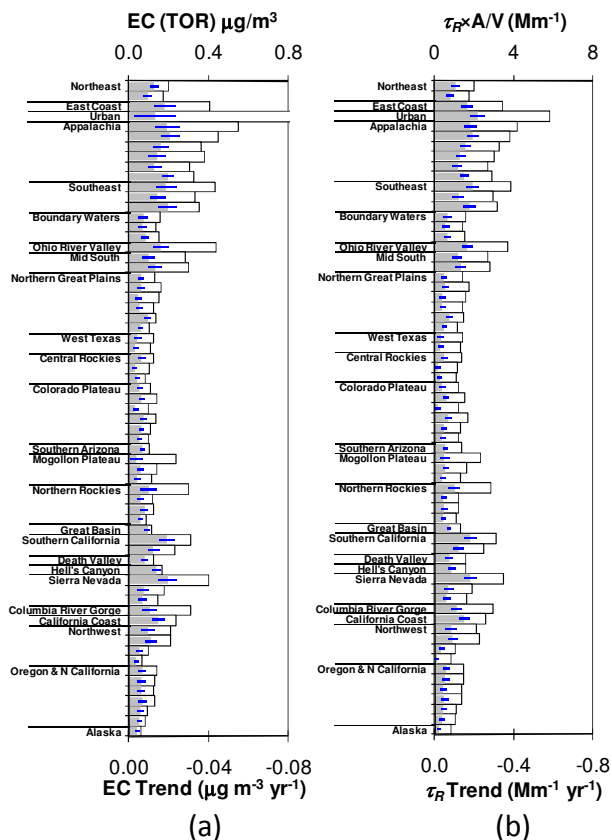


Fig. 6. Median (hollow bar) and trend (solid bar) of **(a)** EC and **(b)** τ_R at 65 IMPROVE sites. See Table 1 for site details. A and V are nominal filter area (3.53 cm^2) and sample volume (32.7 m^3). Medians are those of 2000–2004 baseline period (i.e., EC_{med} and $\tau_{R\text{-med}}$). Trends are based on Sen's slope (2000–2009). The blue bar indicates the 95 % confidence interval of the trend.

Title Page

Abstract Introduction

Conclusions References

Tables Figures

◀ ▶

◀ ▶

Back Close

Full Screen / Esc

Printer-friendly Version

Interactive Discussion

Carbon trends from thermal and optical measurements in the IMPROVE network

L.-W. A. Chen et al.

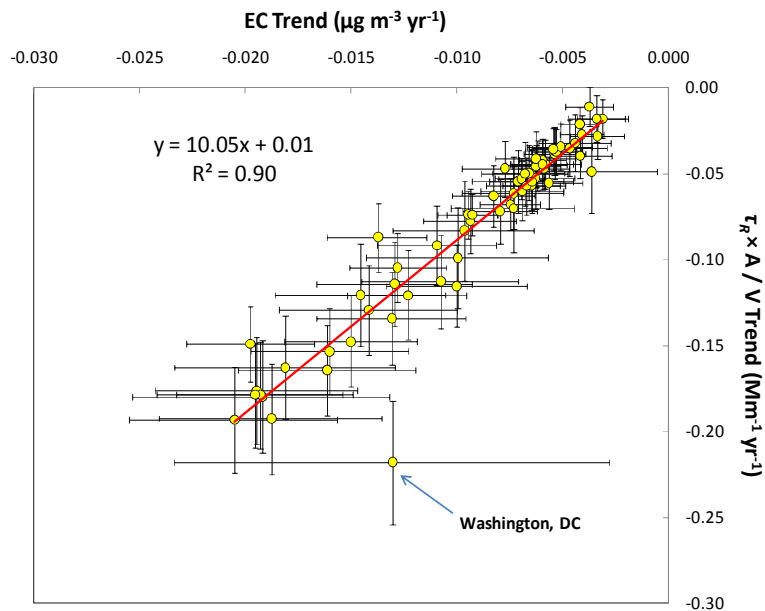


Fig. 7. A comparison of EC and τ_R trends for 65 IMPROVE sites during 2000–2009. A and V are nominal filter area (3.53 cm^2) and sample volume (32.7 m^3). Trends are based on Sen's slope and the error bars represent the 95% confidence intervals.

[Title Page](#)[Abstract](#)[Introduction](#)[Conclusions](#)[References](#)[Tables](#)[Figures](#)[◀](#)[▶](#)[◀](#)[▶](#)[Back](#)[Close](#)[Full Screen / Esc](#)[Printer-friendly Version](#)[Interactive Discussion](#)